International Journal of Innovative Computing, Information and Control
Volume **17**, Number **6**, December **2021**

ICIC International ©2021 ISSN 1349-4198
pp. **2019–2032**

TRAJECTORY FOLLOWING CONTROL FOR AUTONOMOUS VEHICLES USING THE FEEDFORWARD CONTROLLER AND THE IMPROVED TRAJECTORY FOLLOWING MODEL

Jianwei Wu[1,2], Qidi Fu[1], Yanhao Liu[1] and Beibei Sun[1,*]

[1]School of Mechanical Engineering
Southeast University
No. 2, Southeast University Road, Jiangning District, Nanjing 211189, P. R. China
{ wujianwei081x; qidi_fu }@163.com; yanhao.liu@foxmail.com
*Corresponding author: bbsun@seu.edu.cn

[2]School of Mechanical and Electrical Engineering
Guilin University of Electronic Technology
No. 1, Jinji Road, Qixing District, Guilin 541004, P. R. China

Received March 2021; revised July 2021

Abstract. *There are few studies on overall evaluating the effectiveness of a control method when the feedforward controller, the parameters fluctuations, and the states interference are considered, especially when the trajectory following model is changed. For this, this paper proposes an improved trajectory following model considering the computation efficiency, designs a feedforward controller with the linear quadratic regulator (LQR) according to the characteristics of dynamic equations for the trajectory following control, and studies their influence by the comparisons. Furthermore, the trajectory following control is performed by developing the program based on MATLAB language, and the performance by the typical desired trajectory is evaluated using the feedforward controller and the improved trajectory following model. The reliability of the proposed control method is verified from the comparisons of having or not the feedforward controller and of the computational time, and from anti-interference ability and robustness, and simulation results show its superiority.*

Keywords: Trajectory following, Autonomous vehicle, Feedforward control, Improved trajectory following model, LQR

1. **Introduction.** The autonomous vehicle, a highly integrated electromechanical coupling system, is integrated with many vital technologies, one of which is the trajectory following control for tracking the desired trajectory in a continuous and smooth way with the best possible precision [1-4].

Many studies on trajectory following for autonomous vehicles have been carried out in past decades. They mainly focus on applying advanced control algorithms or proposing novel control algorithms including the linear quadratic regulator (LQR) control [5,6], sliding mode control [7-9], neural network control [10-12], and model predictive control (MPC) [13-16], to ensure driving safety and achieve better control effects under the situations that a vehicle model cannot be established accurately and that the uncertain external disturbances exist inevitably. Many of them are to demonstrate the superiority of the proposed method by comparing the response from the different control methods. However, there are few studies on overall evaluating the effectiveness of a control method when the feedforward controller, the parameters fluctuations, and the states interference are considered, especially when the trajectory following model is changed. A large amount

DOI: 10.24507/ijicic.17.06.2019

of literature [13,14,17,18] does not consider feedforward control for reducing the steady-state error; actually, their control effects can be further improved by introducing the feedforward controller.

Therefore, this paper proposes an improved trajectory following model considering the computation efficiency, designs a feedforward controller with the LQR according to the characteristics of dynamic equations for the trajectory following control, and studies their influence by the comparisons. After selecting the typical desired trajectory for simulation control, the performance of the trajectory following control is comprehensively evaluated by considering the feedforward controller, the computational cost, anti-interference ability and robustness.

2. Vehicle Modeling for Trajectory Following Control.

2.1. Vehicle trajectory following model. The vehicle trajectory following model is shown in Figure 1 where C_d is the desired position and C is the real position of vehicle center-of-mass. Point C_d is on the desired trajectory, and vector CC_d and the tangent of C_d are perpendicular. $OXYZ$ is the global coordinate system, $Cxyz$ is the vehicle coordinate system, and $C_dx_dy_dz_d$ is the desired coordinate system in which the tangent of C_d is as the x-axis and the vector C_dC is as the y-axis. In Figure 1, dX and dY are the deviations between points C and C_d in the global coordinate system, φ_{des} and $\dot{\varphi}_{des}$ represent, respectively, the desired yaw angle and yaw rate, V_{xdes} represents the desired longitudinal velocity, and V_x, $\dot{y}$, $\ddot{y}$, φ, $\dot{\varphi}$ and $\ddot{\varphi}$ represent, respectively, the actual longitudinal velocity, lateral velocity, lateral acceleration, yaw angle, yaw rate, and angular acceleration. It is noted that, the magnitude of V_{xdes} and V_x is equal, but their direction is different.

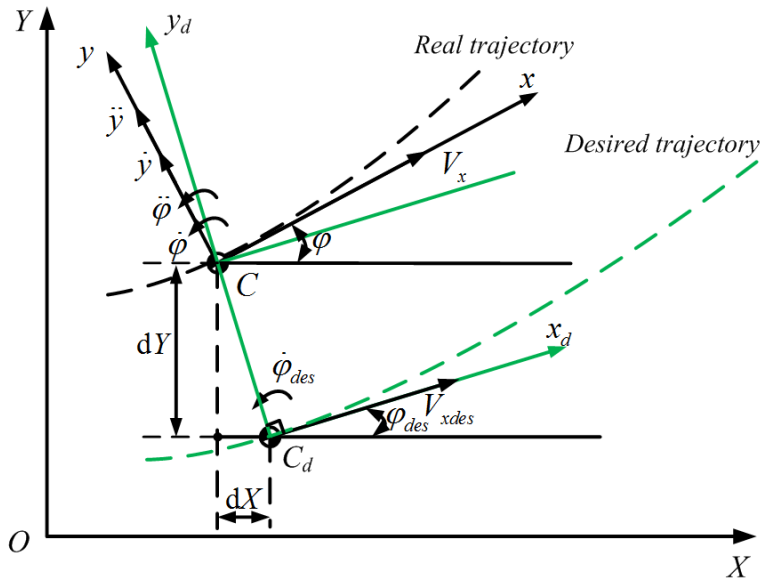

FIGURE 1. Trajectory following model

According to the trajectory following model, the control equation of trajectory following with error form can be obtained as [8]

$$\dot{\boldsymbol{e}} = \boldsymbol{A}\boldsymbol{e} + \boldsymbol{B}\delta_f + \boldsymbol{C}\dot{\varphi}_{des} \tag{1}$$

where

$$\boldsymbol{e} = \begin{bmatrix} e_y \\ \dot{e}_y \\ e_\varphi \\ \dot{e}_\varphi \end{bmatrix} = \begin{bmatrix} y - y_{des} \\ \dot{y} - \dot{y}_{des} \\ \varphi - \varphi_{des} \\ \dot{\varphi} - \dot{\varphi}_{des} \end{bmatrix}, \boldsymbol{A} = \begin{bmatrix} 0 & 1 & 0 & 0 \\ 0 & -\frac{2C_{\alpha f}+2C_{\alpha r}}{mV_x} & \frac{2C_{\alpha f}+2C_{\alpha r}}{m} & \frac{-2l_fC_{\alpha f}+2l_rC_{\alpha r}}{mV_x} \\ 0 & 0 & 0 & 1 \\ 0 & -\frac{2l_fC_{\alpha f}-2l_rC_{\alpha r}}{I_zV_x} & \frac{2l_fC_{\alpha f}-2l_rC_{\alpha r}}{I_z} & -\frac{2l_f^2C_{\alpha f}+2l_r^2C_{\alpha r}}{I_zV_x} \end{bmatrix},$$

$$\boldsymbol{B} = \begin{bmatrix} 0 & \frac{2C_{\alpha f}}{m} & 0 & \frac{2l_fC_{\alpha f}}{I_z} \end{bmatrix}^T, \text{ and } \boldsymbol{C} = \begin{bmatrix} 0 & \frac{-2l_fC_{\alpha f}+2l_rC_{\alpha r}}{mV_x} - V_x & 0 & -\frac{2l_f^2C_{\alpha f}+2l_r^2C_{\alpha r}}{I_zV_x} \end{bmatrix}^T.$$

In these expressions, m is the total vehicle mass, I_z represents the vehicle inertia around the axis Cz, y and y_{des} are, respectively, lateral displacements of the vehicle at the actual and desired point, δ_f is the front steering angle, l_f and l_r denote, respectively, the distances between the front and rear wheel axles with point C, and $C_{\alpha f}$ and $C_{\alpha r}$ respectively represent the front and rear cornering stiffness, and the rest parameters are the same as Figure 1.

If the trajectory following model is performed strictly, it is necessary to solve the nonlinear algebraic equation for calculating the desired point C_d. According to the vertical relationship of tangent of C_d and straight line C_dC for determining point C_d, the nonlinear algebraic equation can be obtained as

$$(Y_C - f(X_{C_d}))\, f'(X_{C_d}) + X_C - X_{C_d} = 0 \tag{2}$$

where X_C, Y_C, X_{C_d}, and Y_{C_d} are the coordinates of points C and C_d, respectively, and $y = f(x)$ denotes the desired trajectory function. However, this equation needs to be solved at each time step, which will reduce the simulation efficiency.

2.2. **Improved trajectory following model.** As shown in Figure 2, an improved trajectory following model is proposed for avoiding solving the nonlinear algebraic Equation (2). This model does not track C_d, but approximates desired point C'_d at next moment. According to the current vehicle states and the planned trajectory, the desired point C'_d at next moment is determined for the error calculation. This handling ensures the steering smoother which is similar to the foresight control.

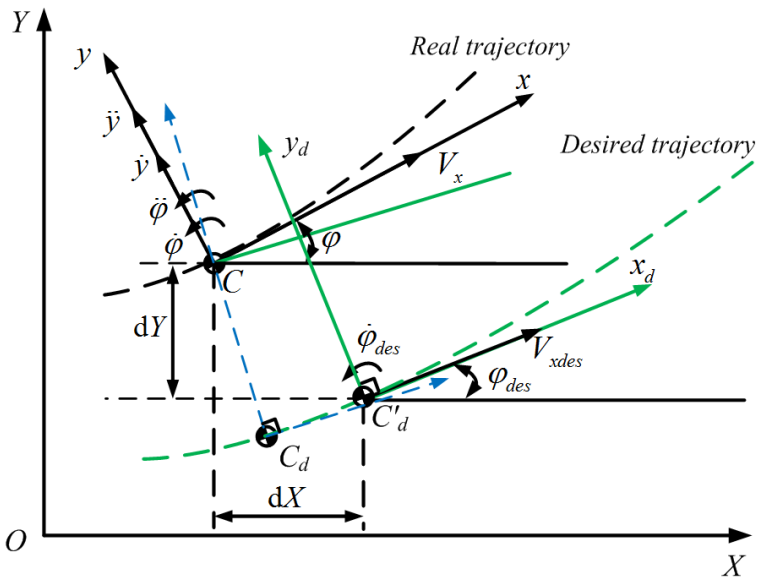

FIGURE 2. Improved trajectory following model

Considering time step h, the next point in the global coordinate system can be approximated as

$$X_{C'_d} = X_C + V_x h + \frac{1}{2} a_x(t) h^2 \tag{3}$$

where $a_x(t)$ is the longitudinal acceleration at moment t.

2.3. **Dynamical equation under the global coordinate system.** When performing trajectory following control on the actual road, an autonomous vehicle needs to accurately measure and estimate the current vehicle states such as the yaw rate, longitudinal velocity, and lateral velocity by a GPS/INS navigation system [14]. Similarly, when performing simulation control for trajectory following, an autonomous vehicle needs to obtain these states by the dynamical equation on the global coordinate system.

This paper mainly focuses on the calculation method of the error for the trajectory following. Therefore, a 3DOF dynamical model for computing the vehicle states is employed, as shown in Figure 3. In this figure, φ represents the attitude of the *Cxyz* with respect to the *OXYZ* (i.e., yaw angle of the vehicle), F_{fy} and F_{ry} respectively denote the y-axis component of the front and rear lateral tire forces with respect to the *Cxyz*, and others are the same as Figure 1. The main assumptions are the following: (i) ignore the difference of tire cornering properties between the left and right wheel due to the load variation, and approximate the tire model as linearity; (ii) assume that the vehicle only performs the front-wheel steering; (iii) assume the longitudinal velocity as a constant value. The vehicle dynamic model is shown in Figure 3 where the origin of *Cxyz* is vehicle centroid and its x-axis is the driving direction.

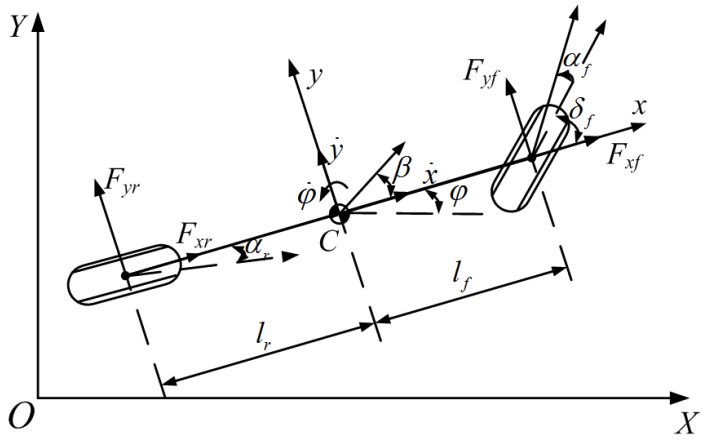

FIGURE 3. Vehicle dynamic model

According to the momentum and moment of momentum theorem under the assumption of longitudinal velocity constant, the dynamical equation under the global coordinate system can be obtained, and its matrix form can be written as

$$\begin{bmatrix} m\ddot{X} \\ m\ddot{Y} \\ I_z\ddot{\varphi} \end{bmatrix} = 2 \begin{bmatrix} -\sin(\varphi) & \cos(\varphi) & 0 \\ \cos(\varphi) & \sin(\varphi) & 0 \\ l_f & 0 & -l_r \end{bmatrix} \begin{bmatrix} F_{fy} + F_{ry} \\ 0 \\ \frac{l_f}{l_r} F_{fy} + F_{ry} \end{bmatrix} \tag{4}$$

where X and Y represent vehicle center-of-mass coordinate with respect to the *OXYZ*.

The transformation relationship between *Cxyz* and *OXYZ* is given by

$$\begin{bmatrix} \dot{x} \\ \dot{y} \end{bmatrix} = \begin{bmatrix} \cos(\varphi) & \sin(\varphi) \\ -\sin(\varphi) & \cos(\varphi) \end{bmatrix} \begin{bmatrix} \dot{X} \\ \dot{Y} \end{bmatrix} \tag{5}$$

F_{fy} and F_{ry} are calculated by the tire side-slip characteristics as [4,19]

$$F_{fy} = C_{f\alpha}\left(\delta_f - \frac{\dot{y} + l_f\dot{\varphi}}{V_x}\right) \tag{6}$$

$$F_{ry} = C_{r\alpha}\left(-\frac{\dot{y} - l_r\dot{\varphi}}{V_x}\right) \tag{7}$$

By substituting Equations (5)-(7) into (4), the dynamical equations under the global coordinate system can be obtained. In the trajectory following control, the steering angle obtained by the controller is used for input of the dynamic equation to obtain the vehicle states at various moments.

It is noted that a large amount of literature [13,14,17,18] does not consider the feedforward control for further improving the control performance. In next section, we will design the LQR control method with the feedforward controller to eliminate the steady lateral error according to the characteristics of the dynamic equation.

3. **LQR Control with the Feedforward Controller.** Assume that the errors $e_y(t)$, $\dot{e}_y(t)$, $e_\varphi(t)$ and $\dot{e}_\varphi(t)$ have been calculated by the following models mentioned in Sections 2.1 and 2.2 according to the desired and actual vehicle states. According to Equation (1) and the LQR control method, the control input $\delta_{f1}(t)$ is obtained by

$$\delta_{f_1}(t) = -\boldsymbol{K}\begin{bmatrix} e_y(t) & \dot{e}_y(t) & e_\varphi(t) & \dot{e}_\varphi(t) \end{bmatrix}^T \tag{8}$$

In Equation (8), $\boldsymbol{K}$ is feedback gain matrix of the optimal control and can be expressed as

$$\boldsymbol{K} = \boldsymbol{R}^{-1}\boldsymbol{B}^T\boldsymbol{P} \tag{9}$$

where $\boldsymbol{P}$ can be obtained by Riccati equation which has the following form

$$\boldsymbol{P}\boldsymbol{A} + \boldsymbol{A}^T\boldsymbol{P} - \boldsymbol{P}\boldsymbol{B}\boldsymbol{R}^{-1}\boldsymbol{B}^T\boldsymbol{P} + \boldsymbol{Q} = \boldsymbol{0} \tag{10}$$

Since the variation of the desired angular velocity results from the different curvatures of the desired trajectory at different times, a feedforward controller is adopted to minimize tracking errors and ensure zero steady-state errors. The autonomous vehicle with only front-wheel steering, belonging to the under-actuated control system, cannot completely eliminate both the steady-state errors from the two states. Nevertheless, it can be ensured that lateral steady-state error is zero, which is more important than angular steady-state error. Next, the feedforward controller – used for completely eliminating the lateral steady-state error – will be introduced in detail, but there still exists angular steady-state error to the under-actuated control system.

According to feedback gain matrix $\boldsymbol{K}$, the closed-loop matrix $\boldsymbol{A}_b$ can be expressed as

$$\boldsymbol{A}_b = \boldsymbol{A} - \boldsymbol{B}\boldsymbol{K} \tag{11}$$

Because the first and third rows of $\boldsymbol{B}$ are zero, regardless of the value of $\boldsymbol{K}$, $\boldsymbol{A}_b$ always satisfies

$$\boldsymbol{A}_b(1,1) = \boldsymbol{A}_b(1,3) = \boldsymbol{A}_b(1,4) = 0,\ \boldsymbol{A}_b(1,2) = 1 \tag{12}$$

$$\boldsymbol{A}_b(3,1) = \boldsymbol{A}_b(3,2) = \boldsymbol{A}_b(3,3) = 0,\ \boldsymbol{A}_b(3,4) = 1 \tag{13}$$

To ensure $\dot{e}_{ys}(t) = \dot{e}_{\varphi s}(t) = 0$ in Equation (1), the relationship between steady-state error and feedforward control can be written as a matrix equation

$$\begin{bmatrix} \boldsymbol{A}_b(2,1) & \boldsymbol{A}_b(2,3) \\ \boldsymbol{A}_b(4,1) & \boldsymbol{A}_b(4,3) \end{bmatrix}\begin{bmatrix} e_{ys}(t) \\ e_{\varphi s}(t) \end{bmatrix} + \begin{bmatrix} \boldsymbol{B}(2)\delta_{f_2}(t) + \boldsymbol{C}(2)\dot{\varphi}_{des}(t) \\ \boldsymbol{B}(4)\delta_{f_2}(t) + \boldsymbol{C}(4)\dot{\varphi}_{des}(t) \end{bmatrix} = \begin{bmatrix} 0 \\ 0 \end{bmatrix} \tag{14}$$

where $e_{ys}(t)$ and $e_{\varphi s}(t)$ denote the lateral and angular steady-state errors at moment t, respectively.

After ensuring $e_{ys}(t) = 0$, the steady-state angular error and feedforward control input at moment t can be expressed as the matrix equation

$$\begin{bmatrix} e_{\varphi s}(t) \\ \delta_{f_2}(t) \end{bmatrix} = - \begin{bmatrix} \boldsymbol{A}_b(2,3) & \boldsymbol{B}(2) \\ \boldsymbol{A}_b(4,3) & \boldsymbol{B}(4) \end{bmatrix}^{-1} \begin{bmatrix} \boldsymbol{C}(2) \\ \boldsymbol{C}(4) \end{bmatrix} \dot{\varphi}_{des}(t) \tag{15}$$

By combining the LQR with feedforward control, the total control input can be calculated as

$$\delta_f(t) = \delta_{f_1}(t) + \delta_{f_2}(t) \tag{16}$$

The control input is not completely determined by Equation (16), and its range should be considered due to the demand for vehicle safety and physical implementation. Here, the ranges of the front steering angle and front steering angle velocity are given by

$$\delta_{\min} \leq \delta_f(t) \leq \delta_{\max} \tag{17}$$

$$\dot{\delta}_{\min} \leq \frac{\delta_f(t) - \delta_f(t - \Delta t)}{\Delta t} \leq \dot{\delta}_{\max} \tag{18}$$

where $\delta_{\min}$ and $\delta_{\max}$ represent the minimum and maximum values of front steering angle, and $\dot{\delta}_{\min}$ and $\dot{\delta}_{\max}$ represent the minimum and maximum values of front steering angle velocity, respectively.

4. Simulation and Performance for the Trajectory Following Control.

To evaluate the feasibility and effectiveness of the trajectory following control, a program is independently developed based on MATLAB language. It is used for implementing trajectory following control, and the simulation results can be shown through solving.

4.1. Desired trajectory.

Before the trajectory following control, a desired trajectory needs to be planned. Currently, several geometric forms could be used for planning the following trajectory. Among them, polynomial trajectories are the commonest form in autonomous driving [20-22]. Therefore, in this paper the cubic polynomial is adopted to express the desired trajectory

$$Y = f(X) = a_3 X^3 + a_2 X^2 + a_1 X^1 + a_0 \tag{19}$$

where a_0-a_3 are the fit coefficients of the cubic polynomial, respectively.

[14] provides a desired trajectory with four radii of curvature which are 180, 100, 150, and 400 m, respectively, as shown in Figure 4. This trajectory has certain representativeness, and this paper will use it to simulate and analyze the trajectory following control.

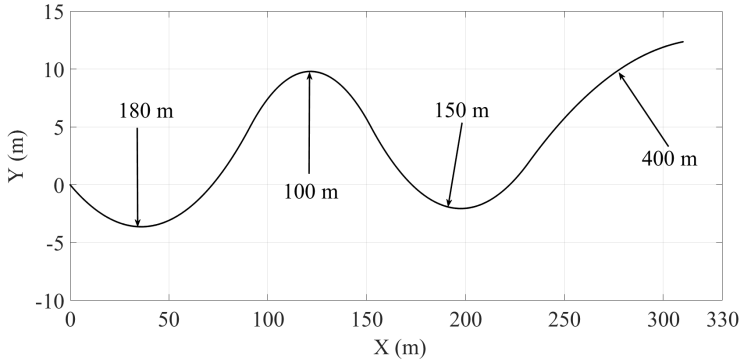

FIGURE 4. Desired trajectory curve planned in advance

TABLE 1. Simulation parameters of the vehicle model

Parameter	Notation	Value
Vehicle mass	m	1800 (kg)
Vehicle yaw moment	I_z	2500 (kg·m^2)
Front-CG distance	l_f	1.03 (m)
Rear-CG distance	l_r	1.49 (m)
Cornering stiffness of front tires	C_f	40000 (N/rad)
Cornering stiffness of rear tires	C_r	40000 (N/rad)
Maximum steering angle	$\delta_{\max}$	0.5236 (rad)
Minimum steering angle	$\delta_{\min}$	-0.5236 (rad)
Maximum steering angle velocity	$\dot{\delta}_{\max}$	0.2618 (rad/s)
Minimum steering angle velocity	$\dot{\delta}_{\min}$	-0.2618 (rad/s)
Longitudinal velocity	V_x	25 (km/h)

4.2. **Vehicle simulation parameters and its initial states.** The simulation parameters of the vehicle model are shown in Table 1.

The initial states are defined as follows. The yaw angle of the vehicle relative to the global coordinate system is -0.2 rad, the yaw rate is 0 rad/s, the lateral and longitudinal velocities are 0 and 25 km/h, respectively. The global coordinate of vehicle center-of-mass is (0 m, 0.2 m).

In the initial states, simulation time is set to 45 s, and the simulation results of trajectory following control can be obtained by using the calculated control input in Section 3.

4.3. **Comparison of simulation results with and without the feedforward controller.** Figure 5 shows the tracking process from the actual vehicle position to the desired trajectory position, and an enlarged partial view is included in it. It shows a good performance for the trajectory following, and the actual vehicle position fluctuates around the desired trajectory at a small scale level.

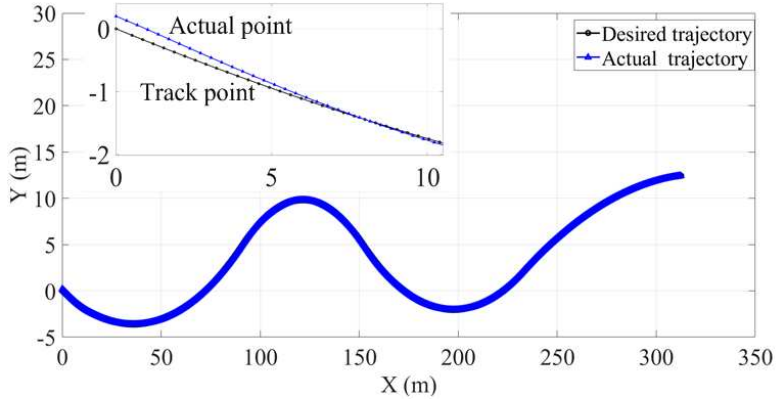

FIGURE 5. The desired trajectory and actual trajectory

Figures 6 and 7 show the responses of lateral and angular errors, respectively. It can be seen from the two figures that by controlling the front steering angle, the lateral and angular errors are gradually reduced, and the desired control effect is achieved. Obviously, the control performance with the feedforward controller is superior to that without feedforward controller, and the steady-states errors with the feedforward controller are smaller. When the vehicle tracks this desired trajectory, the maximum lateral steady-states errors

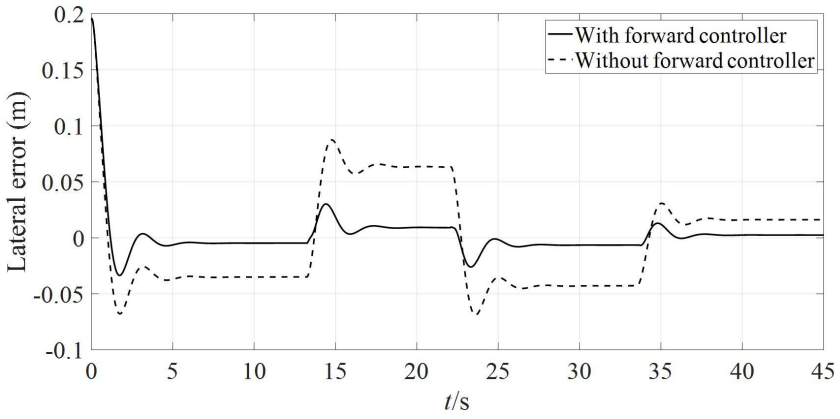

FIGURE 6. Response of lateral error

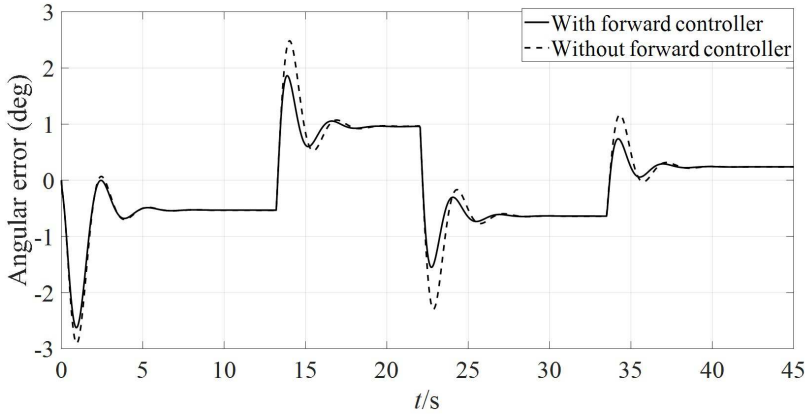

FIGURE 7. Response of angular error

are 0.0636 and 0.0093 m for the control methods without and with feedforward controller, respectively. They are both produced in the position of least radius of curvature. It is noted from Figure 6 that the steady-states error is not completely eliminated, although the feedforward controller is used. The phenomenon can be foreseeable, because the design of the feedforward control is based on the linear dynamical Equation (1), but the simulation model is the nonlinear dynamical Equation (4) under the global coordinate system.

As illustrated in Figure 6, the lateral steady-state error can be greatly reduced, although trajectory curvature is not zero. The simulation results also reveal that when the vehicle passes through the position with small radius of curvature, although the feedforward control has been introduced, its tracking effect will deteriorate to a certain extent. This indicates that the radius of curvature should be enlarged as much as possible when planning the desired trajectory.

Figure 8 shows the response of the front steering angle with and without the feedforward control during the trajectory following simulation. It can be seen that the front steering angle is limited to the given range, which meets the requirements of the vehicle's physical implementability. In addition, the front steering angle is much smaller than the given boundary value (30 deg), and the variation range of the angle with the feedforward controller is smaller than the counterpart without the feedforward controller, which can improve the vehicle's smoothness for tracking the trajectory.

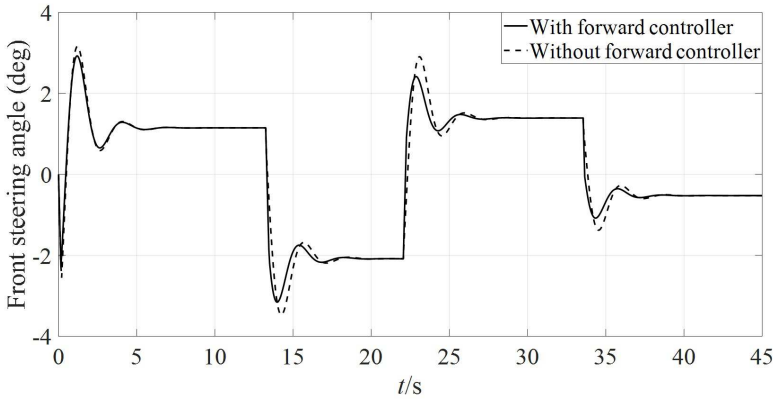

FIGURE 8. Response of front steering angle

It can be seen from Figures 6-8 that, the control performance with the feedforward controller is superior to that without the feedforward controller, and the steady-states errors with the feedforward controller are smaller.

4.4. **Comparison of simulation results from the two trajectory following models.** As we all know, the computation cost is a crucial factor that decides whether the algorithm proposed in this paper can be used in the practice. Accordingly, it is necessary to evaluate the computational cost, and the computer configurations for simulation are as follows.

Operating system: windows 10 with 64 bit
CPU: AMD Ryzen 7 4800H with Radeon Graphics
RAM: 16GB with 3200 MHz
MATLAB version: MATLAB R2018a

In the computing environment, the computation time can be obtained by using timer. When the simulation time is set to 45 s, it is about 0.0441 s for the improved trajectory following model, and 0.8362 s for the trajectory following model. It is noted that the computation time is the average time by repeatedly performing 20 times. Figures 9 and 10 show the called number and time of each function by using the two models for the trajectory following. Because the total time also includes the display time of the interface, it is not the same as the above computation time. It can be seen that the computational cost using the trajectory following model mainly depends on the "fsolve" (i.e., the solution of algebraic Equation (2)), while using the improved trajectory following model does not have this computation cost.

The response of lateral error obtained by the two models is shown in Figure 11. Obviously, the control performance of the improved trajectory following model is superior to that of the trajectory following model, whether it is the lateral error or the calculation time.

4.5. **Anti-interference performance and robustness.** In view of the obvious advantages of using the feedforward controller and improved trajectory following model for the simulation control, the anti-interference performance and robustness are evaluated by using them in this section.

In actual driving, as we all know, due to the uncertain factors such as wind, road condition, and delayed effect from the actuator, the actual vehicle states cannot be consistent with the states calculated by vehicle dynamic model. In addition, the simulation parameters for vehicle dynamic model are not completely accurate under different situations.

Profile Summary
Generated 02-Jul-2021 09:06:34 using performance time.

Function Name	Calls	**Total Time**	Self Time*	Total Time Plot (dark band = self time)
...Driving_PathtrackSimplifyFF_paperguo3	1	1.357 s	0.066 s	
fsolve	900	1.146 s	0.183 s	
optim\private\trustnleqn	900	0.547 s	0.177 s	
optimget	21600	0.205 s	0.080 s	
prepareOptionsForSolver	900	0.138 s	0.112 s	
optimget>optimgetfast	21600	0.125 s	0.125 s	
computeFinDiffGradAndJac	1808	0.122 s	0.042 s	
...rackSimplifyFF_paperguo3>odeADCGNL	3600	0.091 s	0.091 s	
lsqfcnchk	900	0.082 s	0.061 s	
setOptimFcnHandleOnWorkers	900	0.079 s	0.077 s	
finitedifferences	1808	0.077 s	0.040 s	
optim\private\trustnleqn>getOpts	900	0.069 s	0.013 s	
optim\private\dogleg	908	0.044 s	0.044 s	
...tra(x)*(Y(ii+1)-ftra(x))+(X(ii+1)-x))	3616	0.029 s	0.014 s	
finDiffEvalAndChkErr	1808	0.027 s	0.014 s	
createOptionFeedback	900	0.026 s	0.026 s	
isoptimargdbl	1800	0.023 s	0.023 s	

FIGURE 9. Evaluation of the computation time by the trajectory following model

Profile Summary
Generated 02-Jul-2021 09:07:41 using performance time.

Function Name	Calls	**Total Time**	Self Time*	Total Time Plot (dark band = self time)
...Driving_PathtrackSimplifyFF_paperguo4	1	0.164 s	0.020 s	
lqr	1	0.062 s	0.002 s	
...rackSimplifyFF_paperguo4>odeADCGNL	3600	0.058 s	0.058 s	
ss.lqr	1	0.032 s	0.004 s	
ss.ss>ss.ss	1	0.026 s	0.006 s	
care	1	0.020 s	0.005 s	
...tem>DynamicSystem.checkConsistency	1	0.012 s	0.001 s	
gcare	1	0.012 s	0.005 s	
...trackSimplifyFF_paperguo4>ftra_phi	901	0.011 s	0.006 s	
lti.lti>lti.checkDataConsistency	1	0.008 s	0.001 s	
...rackSimplifyFF_paperguo4>curvature	901	0.007 s	0.003 s	
...athtrackSimplifyFF_paperguo4>dftra	3605	0.006 s	0.006 s	
numerics\private\arescale	1	0.004 s	0.002 s	
ssdata.ssdata>ssdata.checkData	1	0.003 s	0.003 s	
...thtrackSimplifyFF_paperguo4>ddftra	901	0.003 s	0.003 s	
...PathtrackSimplifyFF_paperguo4>ftra	901	0.003 s	0.003 s	
ssdata.ssdata>ssdata.checkDelay	1	0.003 s	0.002 s	

FIGURE 10. Evaluation of the computation time by the improved trajectory following model

Therefore, to illustrate the anti-interference performance and robustness of vehicle trajectory following control, Gaussian noises are added in the calculated states by considering the sensor accuracy, and the parameter fluctuations satisfying the uniform distribution is considered in the dynamic equation under the global coordinate system. Here, the front and rear cornering stiffness of the tire and the moment of inertia vary with the uniform

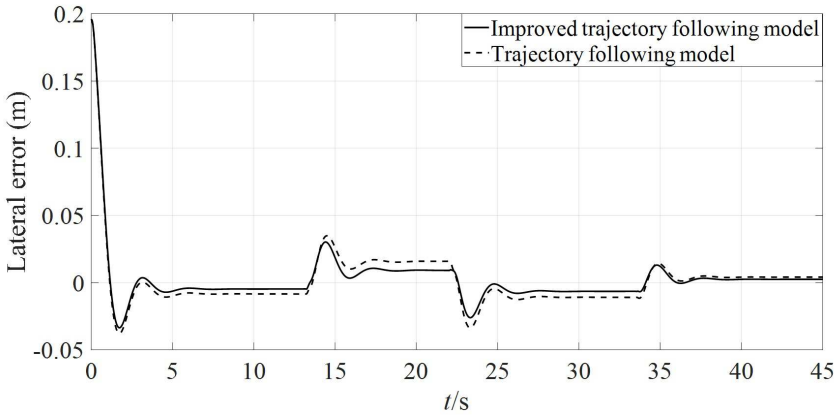

FIGURE 11. Response of lateral error by the two trajectory following models

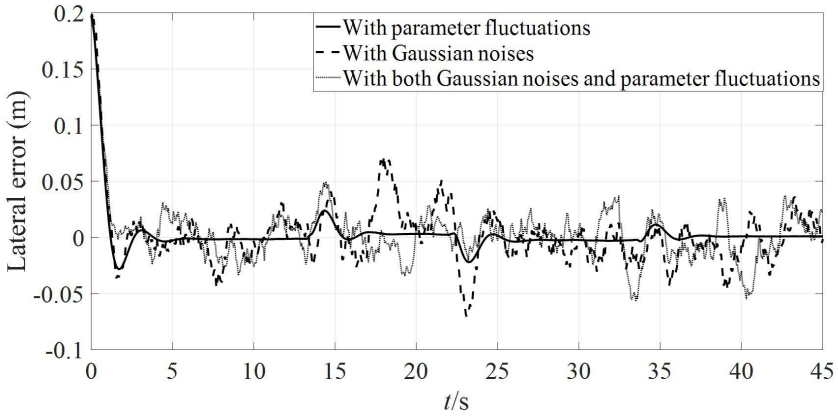

FIGURE 12. Response of lateral error with the uncertainty

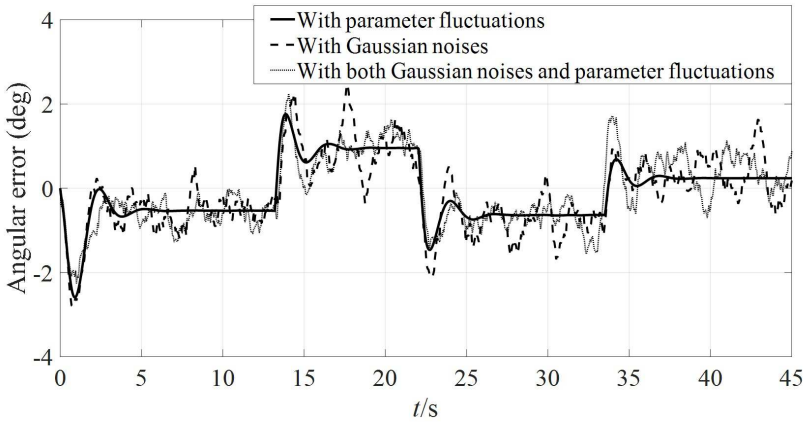

FIGURE 13. Response of angular error with the uncertainty

random distribution, and the range of variation is ± 0.3 times the value shown in Table 1. The robustness of the control can be verified by considering the parameter fluctuations.

The simulation results are shown in Figures 12-14. In the three figures, the solid line represents the response with the parameters fluctuations, the dotted line represents the response with Gaussian noises, and the fine dotted line represents the response with both Gaussian noises and the parameter fluctuations.

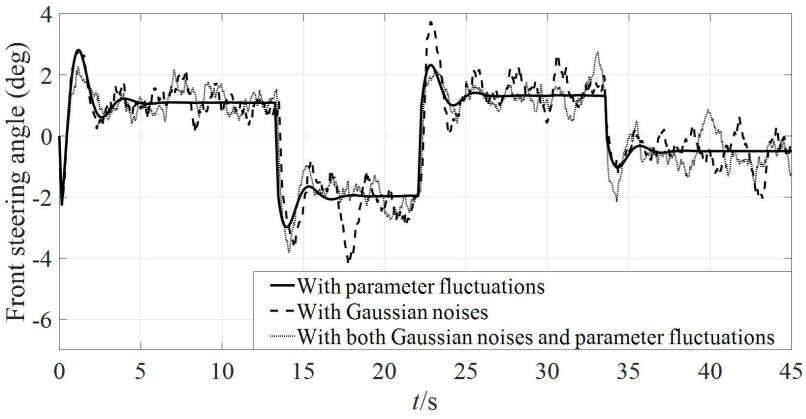

FIGURE 14. Response of front steering angle with the uncertainty

It can be seen that these curves will gradually stabilize to target states under the uncertain disturbance, which demonstrates the good anti-interference performance and robustness of the control method. They also reveal that the influence of control performance from the uncertainty in the given variation range of parameters are not very large. It is noted that the trend of the simulation results considering the uncertainty is the same as that not considering the uncertainty, but they fluctuate along the curves not considering the uncertainty to some extent, which satisfies the actual condition in driving.

The good control performance shows the feasibility and effectiveness of the control method for the trajectory following control, even if the states and the dynamics model of the vehicle have certain uncertainties. Through the above series of evaluations, this control method can be applied in practice.

5. **Conclusions.** This paper proposes the trajectory following control method for autonomous vehicles using the feedforward controller and the improved trajectory following model, on the basis of considering the computation efficiency and the characteristic of dynamic equations for the trajectory following control. The performance of the trajectory following control based on the typical desired trajectory is overall evaluated from the comparisons of having or not the feedforward controller and of the computational time, and from anti-interference ability and robustness. The superiority is verified by the results of the simulation in which a lot of actual situations have been added to demonstrate its strong practicability. It is suggested that the control performance for the trajectory following control should be overall evaluated in other literature to demonstrate the reliability of simulation control method.

Acknowledgment. This research is supported in part by the National Key Research and Development Program of China (Grant No. 2019YFB2006404), and in part by the Guangxi Science and Technology Major project (Grant No. GUIKE AA18242036 and Grant No. GUIKE AA18242037).

REFERENCES

[1] Y. Luo, Y. Xiang, K. Cao and K. Li, A dynamic automated lane change maneuver based on vehicle-to-vehicle communication, *Transportation Research Part C: Emerging Technologies*, vol.62, no.1, pp.87-102, 2016.

[2] X. Li, Z. Sun, D. Cao, D. Liu and H. He, Development of a new integrated local trajectory planning and tracking control framework for autonomous ground vehicles, *Mechanical Systems and Signal Processing*, vol.87, pp.118-137, 2017.

[3] N. H. Amer, H. Zamzuri, K. Hudha and Z. A. Kadir, Modelling and control strategies in path tracking control for autonomous ground vehicles: A review of state of the art and challenges, *Journal of Intelligent & Robotic Systems*, vol.86, no.2, pp.225-254, 2017.

[4] S. Xu and H. Peng, Design, analysis, and experiments of preview path tracking control for autonomous vehicles, *IEEE Trans. Intelligent Transportation Systems*, vol.21, no.1, pp.48-58, 2020.

[5] A. Ortiz, S. Garcia-Nieto and R. Simarro, Comparative study of optimal multivariable LQR and MPC controllers for unmanned combat air systems in trajectory tracking, *Electronics*, vol.10, 2021.

[6] Z. Fan and H. Chen, Study on path following control method for automatic parking system based on LQR, *SAE International Journal of Passenger Cars – Electronic and Electrical Systems*, vol.10, no.1, pp.41-49, 2017.

[7] J. Taghia, X. Wang, S. Lam and J. Katupitiya, A sliding mode controller with a nonlinear disturbance observer for a farm vehicle operating in the presence of wheel slip, *Autonomous Robots*, vol.41, no.1, pp.71-88, 2017.

[8] L. Xu, Y. Wang, H. Sun, J. Xin and N. Zheng, Integrated longitudinal and lateral control for Kuafu-II autonomous vehicle, *IEEE Trans. Intelligent Transportation Systems*, vol.17, no.7, pp.2032-2041, 2016.

[9] A. Chebly, R. Talj and A. Charara, Coupled longitudinal/lateral controllers for autonomous vehicles navigation, with experimental validation, *Control Engineering Practice*, vol.88, pp.79-96, 2019.

[10] G. Han, W. Fu, W. Wang and Z. Wu, The lateral tracking control for the intelligent vehicle based on adaptive PID neural network, *Sensors*, vol.17, no.6, pp.1-14, 2017.

[11] J. Guo, Y. Luo and K. Li, Adaptive coordinated collision avoidance control of autonomous ground vehicles, *Proc. of the Institution of Mechanical Engineers Part I – Journal of Systems and Control Engineering*, vol.232, no.9, pp.1120-1133, 2018.

[12] Y. Chen, C. Lu and W. Chu, A cooperative driving strategy based on velocity prediction for connected vehicles with robust path-following control, *IEEE Internet of Things Journal*, vol.7, no.5, pp.3822-3832, 2020.

[13] Q. Yao and Y. Tian, A model predictive controller with longitudinal speed compensation for autonomous vehicle path tracking, *Applied Sciences-Basel*, vol.9, no.22, 2019.

[14] J. Guo, Y. Luo and K. Li, An adaptive hierarchical trajectory following control approach of autonomous four-wheel independent drive electric vehicles, *IEEE Trans. Intelligent Transportation Systems*, vol.19, no.8, pp.2482-2492, 2018.

[15] J. Hu, S. Xiong, J. Zha and C. Fu, Lane detection and trajectory tracking control of autonomous vehicle based on model predictive control, *International Journal of Automotive Technology*, vol.21, no.2, pp.285-295, 2020.

[16] J. Ji, A. Khajepour, W. W. Melek and Y. Huang, Path planning and tracking for vehicle collision avoidance based on model predictive control with multiconstraints, *IEEE Trans. Vehicular Technology*, vol.66, no.2, pp.952-964, 2017.

[17] J. Guo, K. Li and Y. Luo, Coordinated control of autonomous four wheel drive electric vehicles for platooning and trajectory tracking using a hierarchical architecture, *Journal of Dynamic Systems Measurement and Control – Transactions of the ASME*, vol.137, no.10, 2015.

[18] C. Sun, X. Zhang, L. Xi and Y. Tian, Design of a path-tracking steering controller for autonomous vehicles, *Energies*, vol.11, no.6, 2018.

[19] E. Kayacan, E. Kayacan, H. Ramon, O. Kaynak and W. Saeys, Towards agrobots: Trajectory control of an autonomous tractor using type-2 fuzzy logic controllers, *IEEE-ASME Trans. Mechatronics*, vol.20, no.1, pp.287-298, 2015.

[20] A. Benloucif, N. Anh-Tu, C. Sentouh and J. Popieul, Cooperative trajectory planning for haptic shared control between driver and automation in highway driving, *IEEE Trans. Industrial Electronics*, vol.66, no.12, pp.9846-9857, 2019.

[21] A. Nguyen, C. Sentouh and J. Popieul, Driver-automation cooperative approach for shared steering control under multiple system constraints: Design and experiments, *IEEE Trans. Industrial Electronics*, vol.64, no.5, pp.3819-3830, 2017.

[22] M. Werling, S. Kammel, J. Ziegler and L. Groell, Optimal trajectories for time-critical street scenarios using discretized terminal manifolds, *International Journal of Robotics Research*, vol.31, no.3, pp.346-359, 2012.

Author Biography

Jianwei Wu received the M.S. in mechanical engineering from Guilin University of Electronic Technology, Guilin, China, in 2015. After graduation, he works in Guilin University of Electronic Technology, China. He is currently working toward the Ph.D. degree with Southeast University, Nanjing, China.

His research interests include advanced control strategies and their real-time applications, mechanical/vehicle system dynamics, dynamic optimization for electromechanical system, and noise and vibration control.

Qidi Fu received the B.S. from School of Mechanical Engineering, Changzhou University, in 2017. He is currently studying for a Ph.D. in mechanical engineering at the School of Mechanical Engineering, Southeast University, Nanjing, China.

His research interests include mechanical/vehicle system dynamics, optimum design of structure and noise and vibration control.

Yanhao Liu received the BSc degree in engineering from Southeast University, China, 2019.

Yanhao Liu is currently a postgraduate of the School of Mechanical Engineering, Southeast University, China. His research interests include dynamic analysis and optimal design of mechanical structures, vibration and noise control, and dynamic analysis and control of complex electromechanical systems.

Beibei Sun received the M.S. and Ph.D. degree in mechanical engineering from Southeast University, Nanjing, China, respectively in 1993 and 2001. Since 2008, she has been a Professor with School of Mechanical Engineering, Southeast University, Nanjing.

Prof. Sun is currently a full-time professor at the School of Mechanical Engineering, Southeast University, China. Her current research interests include design/control of vehicle dynamics, noise and vibration control, and dynamic optimization for mechanical system. She is a reviewer for several academic journals related to vehicle dynamics, noise and vibration control and dynamical optimization. She has published over 100 papers in journals and conferences. She has presided over many research projects funded from National Natural Science Foundation of China.